Development of Miniaturized Pneumatic Artificial Muscle for Surgical Device

Shanthanu Chakravarthy, Aditya K. and Ashitava Ghosal
Department of Mechanical Engineering
Indian Institute of Science
Bangalore, India
{sc, adityak, asitava}@mecheng.iisc.ernet.in

***Abstract*— Robotic surgical tools used in minimally invasive surgeries (MIS) require reliable actuators for precise positioning and control. Miniature pneumatic artificial muscles (MPAM) appear most suited for actuating surgical devices because of their inert nature, high force to weight ratio and fast actuation. However, MPAMs are not readily available and pose considerable challenge in their design and control. In this regard, we develop a miniaturized air muscles with outer diameter of ~1.2 mm. The developed MPAMs have high contraction ratio of about 22% and can provide pull force in excess of 5N at a supply pressure of 0.83 MPa. In this paper, we present the details of the developed experimental set-up, experimental data on contraction and force as a function of applied pressure and characterization of the MPAM. Furthermore, the details of the design and experiments with novel endoscopic surgical tool that uses the developed MPAMs for improved dexterity and position control are presented.**

Keywords —: Mckibben actuators, Micro-actuator, endoscopic surgery.

I. INTRODUCTION

There is a large requirement for micro actuators with capability of precise positioning and control in applications such as surgical tool used in minimally invasive surgery. Pneumatic Artificial Muscles (PAM) are pneumatic actuators that generate tensile forces, preserving properties such as compliance, robustness, biological inertness and these make them suitable for in-vivo operation [1-5]. The conventional PAM's such as those used for robotic and industrial applications require high pressure and are too large to be used in surgical tools used for minimally invasive surgery. Conventional PAM's have non-linear characteristics, are difficult to integrate in mechanical design but are advantageous due to their air-tight design and low cost fabrication.

Endoscopes are minimally invasive surgical tools that are commonly used for imaging and diagnosis in the gastro-intestinal tract and are increasingly being used for procedures such as biopsy. A typical endoscope consists of 12 mm diameter flexible tube with a length of 100 cm to 250 cm and carries a camera and imaging system at the end. The endoscope also has channels through which a fiber optic cable, air, water and small end-effectors such as a scissors can be made to pass. The tip of the conventional endoscope can bend to provide various viewing angles. The bending is achieved by universal joints which are actuated by wires connected to a thumb wheel operated by the surgeon. The endoscope is relatively flexible due to the wire actuation mechanism and therefore precise operation of the surgical tool is difficult in complex shaped areas. Due to the large flexibility it is also difficult to precisely position scissors and other end-effectors used for biopsy or other minute surgical procedures. A way to overcome this problem is to develop mechanisms which can be flexible and at the same time can be made stiff to precisely position the end-effectors. This, however, require the use of miniature actuators and several attempts were made by researchers in developing the micro actuators for surgical tool applications [6].

Ikuta et al [7] developed a five segments actuated with shape memory alloy (SMA) servo actuator system. However, this actuator required high currents and the actuation is slow. Choset [8] developed a design with two concentric tubes consisting of a series of cylindrical links connected by spherical joints. In this design these joints cannot be actuated independently, slow forward speed and large external feeding mechanism is required. Simaan et al [9] developed a four-degrees-of-freedom snake like arms actuated by SMA wires. The flexibility of the snake robot is limited by the length and diameter of the rigid members and requires complex control strategies. The laboratorie de Robotique de Paris (LRP) developed a 8 mm in diameter snake like mechanism, formed by a sequence of segments and articulated by SMA actuated pin joints[10]. Hirose [11] also used an SMA spring and wire actuation to make a small surgical device; the novelty of this mechanism is to overcome the hysteresis commonly found in SMA's. Lim et al [12] developed a 2.8 mm in diameter active catheter based on silicon micromachining. This multilane manipulator is connected by joints made of SMA, fixed at equilateral triangles locations to allow bending in several directions. In summary, SMAs can be used to actuate joints and offers the possibility of developing micro-actuators required for surgical instruments. The main drawbacks are the use of high activation voltage and slow response time. Researchers at Pennsylvania State University [13] have

This work was financially supported by the Robert Bosch Centre for Cyber Physical Systems (RBCCPS) at the Indian Institute of Science (IISc), Bangalore.

also developed snake-like manipulator using electro active polymer artificial muscle (EPAM) which allows the control of the curvature. Much of these works have focused on developing a new form of actuation using EPAM [14].

The scope of this research is to develop a miniaturized pneumatic artificial muscle (MPAM) of approximately 1 mm thickness and to characterize its properties. The aim is to use these PMAM in developing actuators for surgical tool with two degree of freedom. In Section 2, the working principle of the pneumatic artificial muscles and its fabrication is presented. Section 3 presents the static modeling of the pneumatic muscles. Experimental setup for the complete characterization of the developed MPAM, experimental results is discussed in Section 4. In Section 5 we develop the control architecture together with robust controller and validation its performance on the system. In section 6 we present the development of the endoscopic surgical device and initial experiments with the same. Final concluding comments and future work are discussed in section 7.

II. PNEUMATIC ARTIFICAL MUSCLE(PAM)

There are two primary components of a pneumatic artificial muscle (PAM). One is the soft, stretchable inner rubber tube (generally silicone tube) and the other is braided nylon mesh sleeve (see Fig 1). The physical properties of the braided mesh is to control the over inflation of the pressurized silicone tube and prevent its rupture, convert large radial expansion into axial contraction, and setting limits of stretch and contraction. Schulte et al [15] shows that a limit of contraction occurs at braid angle of 54.7º. The contraction of a PAM is similar to a biological muscle and hence the name pneumatic artificial air muscle.

A. *Fabrication MiniaturizedPneumatic Artificial Muscle(MPAM)*

The components that are required for manufacturing of MPAM'S are platinum cured silicone tube, braided nylon mesh sleeve, micro pipette, nylon tubing, glue, zip tie and a surgical thread. The silicone tube is custom manufactured by a foreign manufacturer and has an inner diameter of 0.5 mm and outer diameter of 0.9 mm. Before braiding, the silicone tube is pre-stretched several times by pressurizing the silicone tube and releasing the pressure. This process relives the bias in the silicone tube and results in uniform expansion of the tube. After this process a nylon mesh is tailored on the pre-stretched silicone tube. The wire diameter of nylon braided sleeve is around 0.1mm. Finally one end of the MPAM is knotted using surgical thread. The other end of the MPAM is attached to a conical connector and wrapped with surgical thread to make it more air-tight. Fig 2 shows the fabricated MPAM. The thickness of the developed MPAM, shown in Fig 2, is around 1.2 mm and length is around 130 mm. Different length MPAM's can be manufactured by varying the length of the silicone tube.

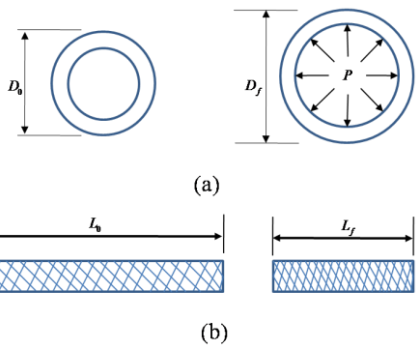

Fig 1: (a) Cross sectional view of the silicone tube before pressurizing and after pressurizing, (b) Behavior of the braided sleeve before contraction and after contraction.

III. STATIC MODEL OF THE MPAM

The static model of pneumatic actuators was developed by Chou and Hannaford [1]. Alternatively, the behavior of the pneumatic actuators has been modeled by the Colbrunn et al [4]. In his modeling, PAM is modeled as a cylinder by ignoring the non- cylindrical effects and wall thickness. The static relation between the length of the PAM and the forces exerted by the actuator is given by,

$$F = \frac{P b^2}{4\pi n^2}\left(\frac{3L^2}{b} - 1\right) \quad (1)$$

where L is the length of the actuator and P is the pressure applied to the PAM. Other geometric parameters are constants thread length b, the number of turns n of a single thread and the interweave angle θ. These geometric parameters are shown in Fig 3.

Equation (1) is a simple analytical expression obtained from the principle of virtual work. However, this equation

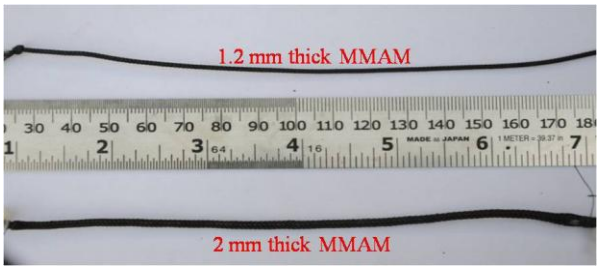

Fig 2: Fabricated miniaturized pneumatic artificial muscle (MPAM)

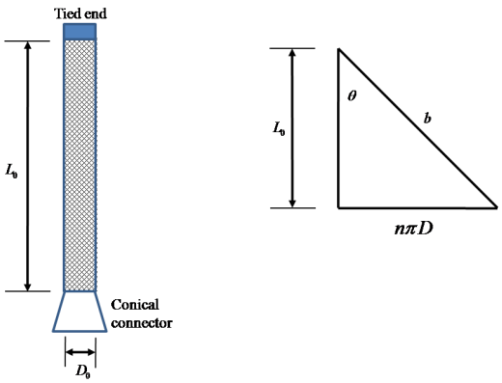

Fig 3: Modeling of MPAM

does not take into account the friction in the braids and slip between the braid and silicone tube. In this work, we use the model of Tondu and Lopez [16]. Their model has a tuning parameter to account for the unmodeled friction and slip.

The relation between the force, F and contraction ratio of pneumatic muscle, $\in$ with respective to pressure, P is given by,

$$F_{(\in,P)} = \left(\pi r_o^2\right) P\left(a(1-k\in)^2 - b\right), \quad 0 \le \in \le \in_{\max}$$

$$\text{where,} \quad \in = \frac{(l_o - l)}{l_o} \text{ and} \tag{2}$$

$$a = \frac{3}{\tan^2(\theta)}$$

$$b = \frac{1}{\sin^2(\theta)}$$

Where r_o is defined as the radius of the inner tube which is in contact with the braided sleeve, l_o is the initial length of the muscle, $\theta = 38.97^o$ is the interweave angle between the braided fibers. The fiber angle is determined by using a microscope and imaging technique as shown in the Fig 4. When the air muscle contracts, it forms a conical shape at both ends and hence the active part decreases. Fig 5 shows the force versus contraction ratio curves obtained using equation (2). These results were obtained for a pneumatic muscle with outer radius 0.5 mm and length 100mm. The actual contraction ratio is smaller than expected. The tuning parameter which matches the experimental characteristics was found to be $k = 0.9$ for the MPAM tested in this work.

It should be noted here that that, the models presented here are approximate. A more accurate modeling can be achieved by Finite Element Analysis (FEA). However, FEA for PAM is more involved and is not in the scope of this work.

IV. EXPERIMENTAL SETUP FOR CHARACTERIZING MPAM

The fabricated MPAM actuator is characterized for contraction in length and the pull force as a function of applied pressure. Fig 6 shows the experimental setup used for static characterization of MPAMs. It consists of an air

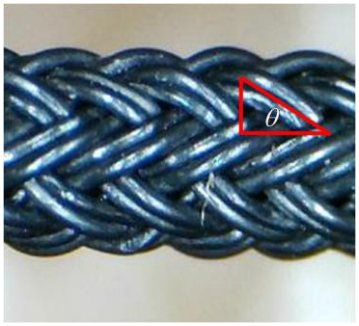

Fig 4: Braid angle measurement using microscope

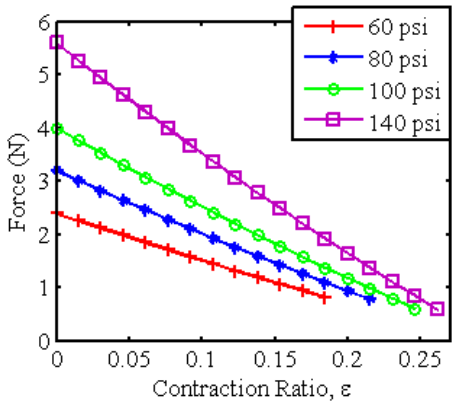

Fig 5: Force versus contraction graph obtained using analytical model

compressor capable of a maximum output of 150 psi, a reservoir, air muscle of thickness ~1.2 mm, and standard weights (10g, to 600 g) to apply axial loads. A silicon pressure transducer manufactured by Honeywell (0 to 150 psi input) is used to measure the pressure. An infrared displacement sensor (range of 4 cm to 30 cm) manufactured by SHARP is used for measuring the contraction of the MPAM. The setup consists of a pulley system to apply axial forces using standard weights. Two proportional valves (VSO series manufactured by Parker Inc) are used to control the pressure by applying voltages to the valves. One of the valve acts like an inlet valve for the inflation of the air muscle and the other valve acts like bleed valve. An ardunio 2560 board is used as a data acquisition device taking the readings from the pressure transducer and displacement sensor.

A. *Results and Discussion*

During the experiments, one side of the MPAM is fixed to a block using a clamp and a wire is tied to the free end of the air muscle. The wire from the free end of the MPAM is looped around the pulley for hanging weights. A small plate is also attached to the wire and a white paper sheet is pasted on to the plate to act as an obstacle for the

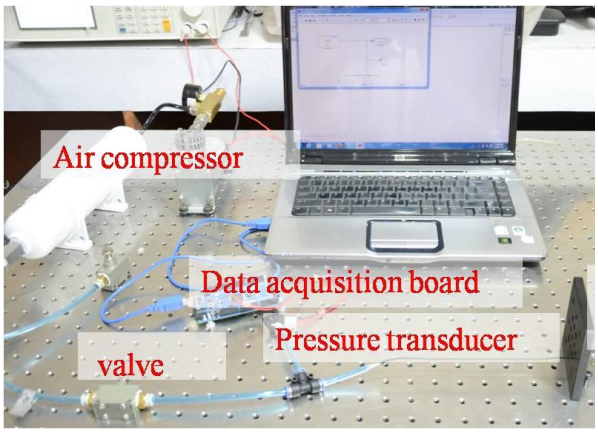

Fig 6: Experimental setup designed for the characterization of MPAM.

displacement sensor. Different weights were suspended and the contraction and force generated by the air muscle are measured for different pressures. Numerous experiments were carried out to characterize the fabricated MPAM. Fig 7(a) shows the plot of contraction versus force developed in a 10 cm long MPAM. We observe that up to 5 N force can be obtained during contraction. Fig 7(b) shows the contraction as pressure is increased and decreased. As can be seen in Fig 7 (b), there is some hysteresis. This hysterics has to be accounted during the actuation of the muscle. The force-contraction results are reasonably good and it shows that we get ~ 25 % contraction. This contraction is reasonably good compared to SMA actuation and hence we can use the MPAM for constructing a surgical tool.

Experiments were also conducted for obtaining the maximum force generated by the MPAM. This is shown in the Fig 8. Commercially available load cell is used for measuring the force generated by the actuator. The graph shows that at least 5N of force can be obtained as the pressure approaches 120 psi.

V. Control Architecture

One of the difficulties in using PAM is the control of pressure in the pneumatic circuit. To actuate the MPAM developed in this work, we have implemented a control strategy based on Sliding Mode technique. The block diagram of the controller is shown in Fig 9. A pressure regulating switch, switches on/off the air compressor to maintain the set pressure in the reservoir. Pressure to the pneumatic muscle is supplied through the reservoir and controlled using a proportional valve (miniature VSO proportional valves manufactured by Parker. Inc). A feedback controller is designed to set the pressure in the pneumatic muscle to a desired value. The controller receives the feedback signal of the measured pressure in the pneumatic muscle and gives the output voltage to drive the proportional value. The entire instrumentation and controller is implemented on an Arduino mega 2560 board that is programmed to serially transmit sensor data. These transmitted data was captured using a computer for analysis and controller tuning. Because all the controller computations are carried out in the Arduino's processor board itself, there was very little transmission delays.

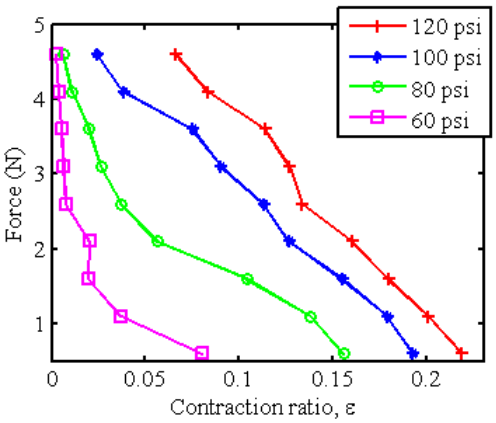

(a)

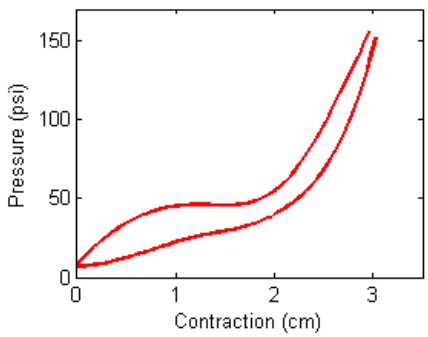

(b)

Fig 7: (a) Force versus contraction ratio plot for the developed MPAM, (b) Hysteresis exhibited by the MPAM at 0.5 N load

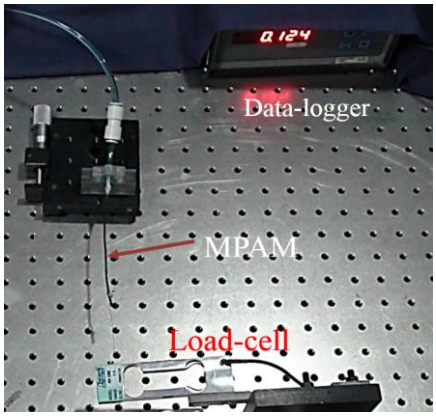

(a)

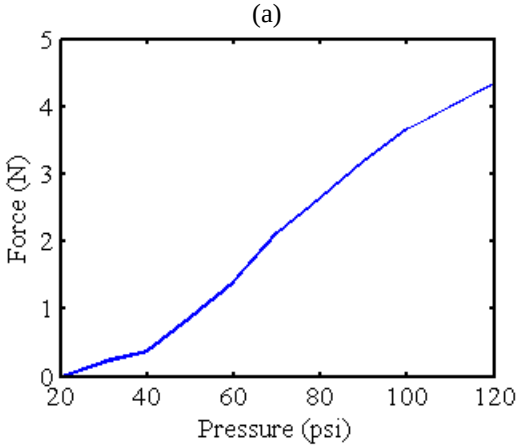

(b)

Fig 8: (a) Experimental setup for obtaining maximum force generated by the MPAM, (b) Forces versus pressure for the MPAM

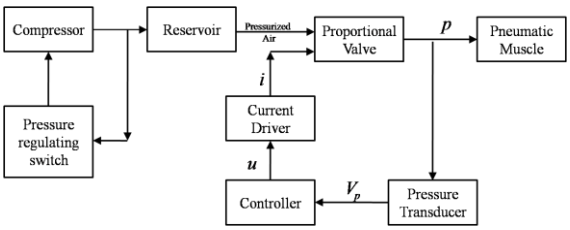

Fig 9: Control architecture for controlling the developed MPAM

During our experiments we found out that Arduino is able to efficiently handle all the instrumentation and control computations when the control loop was set to operate at 1 KHz.

Arduino Mega board used in our experiments can output PWM voltages in the range of 0-5 V with maximum current of 40 mA. However, the proportional valves used in our experiments are solenoid valves that are driven by current signals. To drive these valves using Arduino's 0 -5 V voltage range, a current driver circuit was designed and a PCB for the same was manufactured. The current driver circuit is based on LM 358 IC and draws a maximum current of 1 mA. The circuit diagram of the designed driver circuit is shown in Fig 10.

A. Controller Development

In this sub-section, we report the initial simplified approach used to develop the controller and tune the gains heuristically. Elementary system identification was carried out by giving a step input to the system. A step in voltage is given to the driver circuit and pressure in a 10 cm long pneumatic muscle was noted. We observed from our experiments that the system is fast and has a time constant of ~ 0.09 s and the system was damped with no overshoot. We fit a first order model to the system based on the step response. This model was used to design a PID controller using MATLAB/SIMULINK simulations.

However, we noticed that the controller performance in the actual system was not satisfactory and varied with different step size and back pressure. The reasons for this discrepancy can be attributed to the uncertainties caused by nonlinearities in the system. For developing a robust controller, for taking care of the uncertainties, a sliding mode control (SMC) scheme [17] was developed. This is described in brief next.

The SMC is formulated based on the error, e, which is the difference between the feedback and set pressure values. If p_d is the desired pressure and p_m the measured pressure, then the error, $e = p_d - p_m$. The desired pressure values are specified by the inverse kinematics of the device

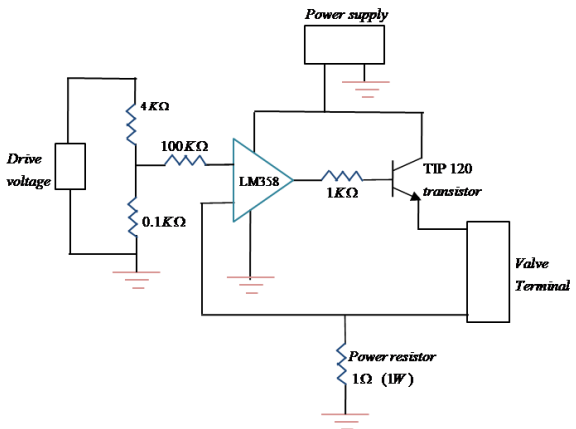

Fig 10: Current driver circuit for the proportional valve

and the static pressure versus contraction maps presented in Section 4.

The dynamics of the sliding mode controller is defined by the sliding manifold, S, where,

$$S(e,t) = 0 \tag{3}$$

Choosing the sliding surface to be a function of error, e and adding an integrator to remove steady state error, we get

$$S = e + K_i \int e\,dt \tag{4}$$

Now we employ Lyapunov stability theory to determine the stability of the controller [17]. Consider a Lyapunov function, V_L which is positive definite and continuously differentiable.

$$V_L = \frac{1}{2} S^2 \tag{5}$$

Taking derivative with respect to time and substituting from equation (4)

$$\dot{V}_L = S\,\dot{S}, \quad or \quad \dot{V}_L = S\,(\dot{e} + K_i\,e) \tag{6}$$

Now, consider the first order linear model estimated by open loop experiment. All the unmodeled dynamics and the uncertainties can be lumped into a function, $h(p,u)$ and added into the first order model estimate. The approximate state equation can now be written as:

$$\dot{P} = g(p) + h(p,u) + u \tag{7}$$

Any uncertainty associated with u is also lumped into $h(p,u)$ to make u as linear input to the approximate state equation (7). It is noted from experience that all the uncertainties associated with the control input are small enough to retain control authority. Substituting the state equation into Lyapunov function gives,

$$\begin{aligned} \dot{V}_L &= S\,[\dot{P}_d - \dot{P}_m + K_i e], \ or \\ \dot{V}_L &= S\,[\dot{P}_d - g(p) - h(p,u) - u + K_i e] \end{aligned} \tag{8}$$

Choosing control law to cancel unknown nonlinear functions, we get

$$\begin{aligned} &u = A - \beta\, sign(S) \\ &where,\ A = -\dot{P}_d + g(p) + h(p,u) - K_i e \end{aligned} \tag{9}$$

For the control system to be stable in the sense of Lyapunov, equation (8) has to be negative definite and the following condition should hold for all time, t, i.e., we need

$$\beta \geq A \tag{10}$$

Since all the terms in A are difficult to estimate and characterize, we set β to a large value heuristically to make equation (8) negative definite over a large range of operation. In order to avoid the chatter associated with SMC we implemented the continuous form of the controller given by,

$$u = A - \beta \tanh\left(\frac{S}{\varepsilon}\right) \qquad (11)$$

B. *Controller Validation*

In this section, we validate and characterize the performance of the robust controller derived in the previous section to set the desired pressure in the MPAM. A step input to set the pressure in MPAM to 80 psi is given to the controller. Fig 11(a) and 11(b) shows the step response of the controller for two different β values 120 and 150. The time constant of the controller response is found to be ~0.06 s. By choosing β to be 150, the response time can be further reduced to 0.01 s with a small increase in overshoot (~7%). We also note that any small leak in the pneumatic circuit conditions the flow and aids in obtaining high control accuracy with a small sacrifice of response time.

VI. Design of Articulated Endoscopic Surgical Device

Once the MPAM and the controller was developed and characterized, we next developed concepts for an articulated endoscope. This section describes initial attempts and the work is continuing.

Fig 12 shows two possible concepts for an articulated and actuated endoscope. Fig 12 (a) shows 5 rigid rings each with an outer diameter on 12 mm. In the rings, there are 3

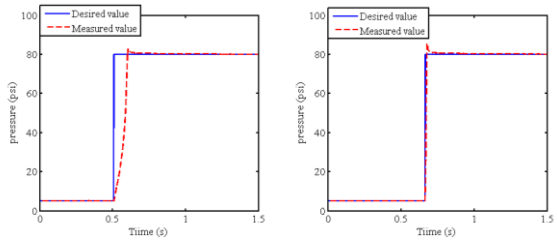

Fig 11: (a) Controller response for gain 100**,** (b) Controller response for gain 150

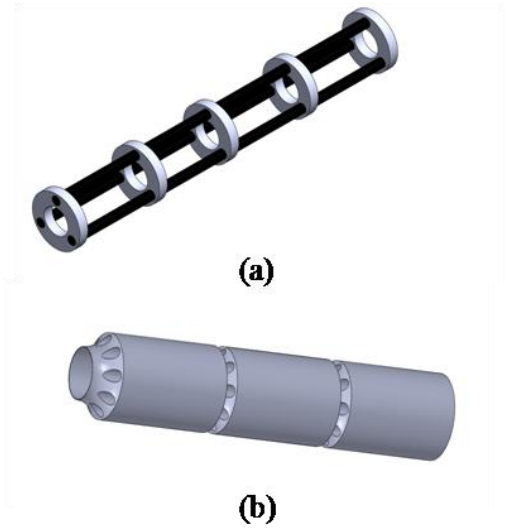

Fig 12: Two conceptual designs of actuated links of an endoscope

holes of diameter 2.2 mm spaced 120 degrees apart. Through the holes, we pass three braided MPAMs which give some flexibility to the assembly. As the air muscles are pressurized, they will contract and entire assembly of rings and MPAM will move. Depending on which of the three (or which two) MPAM is pressurized, the assembly will move in 3D. Thus this arrangement serves as a two-degree-of-freedom Hook joint. Fig 12 (b) shows three rigid cylindrical pieces. The cylinder walls have holes of appropriate diameter through which MPAMs can be inserted. The cylindrical pieces fit like a cup and cone and as the MPAMs are pressured in a selective manner, there will be relative motion between the two rigid cylinders. Again by appropriately pressuring one or more MPAM in the set of three MPAM, we can achieve an actuated two-degree-o-freedom joint. In Fig 12 (b), three joints and links are shown. In an actual actuated endoscope, 6 or more joints will be required.

We have fabricated a device similar to the one shown in Fig 12 (a). The operation of which, is shown in Fig 13. Our device consists of 12 mm diameter spacer discs with three 120^{o} spaced peripheral holes. MPAMs are inserted through the peripheral holes of the closely spaced spacer discs. The diameter of the peripheral holes is 2.2 mm to allow for easy inserting and small expansion during actuation of MPAMs. A 4 mm hole in the center of each spacer disc relieves space for inserting fiber optic camera and other surgical tools (like scissors, biopsy tool). For the prototype, the spacer discs were manufactured using a rapid prototyping process. Fig 13 shows snapshots of the endoscopic surgical device as the air pressure is applied to the MPAMs. These snapshots are extracted from a video showing motion of the endoscope.

One joint in our proposed endoscopic device is actuated by three pneumatic muscles. All the pneumatic muscles actuating the endoscopic device take pressurized air from the same line and are individually controlled by proportional valves. To do position tracking of the entire endoscopic surgical device, the MPAMs have to be inflated and deflated in a controlled manner. This requires two proportional valves for each MPAM actuator, one for inflating and another for bleeding to the atmosphere. However, using two valves for each pneumatic muscle causes the actuation scheme to be redundant. Control of

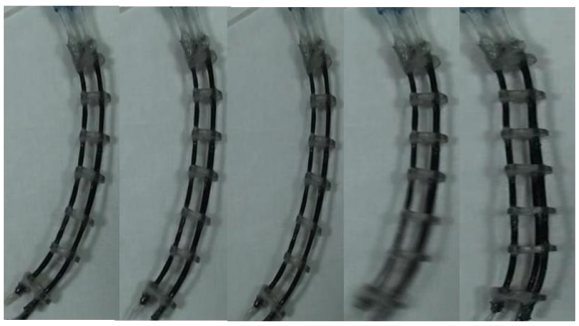

Fig 13: Snapshots showing the rotational motion of the endoscopic surgical device.

redundant actuators is more involved and requires a centralized control scheme for control allocation and work on this aspect is continuing.

VII. CLOSURE

An efficient and reliable miniature pneumatic actuators and their control is presented in this work. Characterization of the fabricated MPAM showed that the actuators can provide high force (~5 N) when operating at a maximum pressure of 0.83 MPa. A robust control scheme based on sliding manifold is derived for controlling pressure in the MPAMs. The controller is robust against uncertainties and has fast response (~0.01 s). We have also proposed an endoscopic surgical tool actuated by MPAMs. Future research will focus on complete characterization of MPAM and development of an accurate model based on FEA. We are also working on improving the proposed endoscopic surgical device with continuous tracking control capability and with several links.

ACKNOWLEDGEMENTS

We would like to thank Professor. G. K. Ananthasuresh for providing us lab facilities and Raghavan and his team of Electrical & Allied Products for providing customized braided sleeve. We would also like to thank Ramu G for helping us in design and rapid prototyping.

REFERENCES

[1] C.P Chou, B Hannaford, ``Static and dynamic characteristics of pneumatic artificial muscles'', Proc of IEEE International conference on Robotics and Automation , Vol.1, pp. 281-286, 1994.

[2] D.Cadwell, G..Medrano-Cera and M. Goodwin, ``Control of pneumatic muscle actuators'', IEEE Control Magazine, Vol.15, pp. 20-30, 1995.

[3] C. Chou and B. Hannaford, ``Measurement and modeling of pneumatic artificial muscles'', Proc.of IEEE International Conference on Robotics and Automation, Vol.12, pp. 90-102, 2002

[4] R. Colbrunn, G. .Nelson and R. Quinn, ``Design and control of robotic leg with braided pneumatic actuators'', Proc. Of IEEE/RSJ International Conference on Intelligent Robots and Systems, Vol.2, pp. 992-998, 2001.

[5] K. C. Wickramatunge and Thananchai Leephapreeda, ``Study on mechanical behaviors of pneumatic artificial muscle'', International Journal of Engineering Science, Vol.48, pp. 188-198, 2002.

[6] M. l. De Volder, A. Moers and D.Reynaerts, ``Fabrication and control of miniature pneumatic actuators'', Sensors and Actuators A:Physical, Vol.166, pp. 111-116, 2011.

[7] K. Ikuta, M. Tsukamoto and S. Hirose, ``Shape memory alloy servo actuator system with electric resistance feedback and application for active endoscope'', Proc. of IEEE Int. Conference on Robotics and Automation Philadelphia, Vol. 1 pp. 427-430, 1988.

[8] T. Ota, A. Degani, D. Schwartzman, B. Zubiate, J. McGavery, H. Choset and M. A. Zenati, ``A highly articulated robotic surgical system for minimally invasive surgery'', Ann. Thoracic Surgery, Vol. 87, pp. 1253-1256, 2009.

[9] K. Xu, R. E. Goldman, J. Ding, P. K Allen, D. L Fowler and N. Simaan, ``System design of an insertable robotic effector platform for single port access(SPA) surgery'', Proc. of IEEE/RSJ Int. Conf. Intelligent Robotic Systems, pp. 5546-5552, 2009.

[10] J. Szewczyk, V.de Sars, P. Biduad and G. Dumont, ``An active tubular poly articulated and micro system for flexible endoscope'', in Lecture Notes in Control and Information Sciences, Vol. 271/2001, Experimental Robotics VII: Springer -Verlag, pp. 179-188, 2003.

[11] S. Hirose, ``Biologically inspired robots: snake-like locomotors and manipulators'', Applied Mechanics Reviews, Vol. 48, no. 3, pp. 27, 1995.

[12] G. Lim, K. Minami, K.Yamamoto, M.Sugihara, M.Uchimaya and M.Esashi ``Multi-link active catheter snake-like motion'', Robotica, Vol. 14, no.5, pp. 449, 1996.

[13] M. I. Frecker and W. M. Aguilera, ``Analytical modeling of a segmented unimorph actuator using electrostrictive (PVDF-TrFE) copolymer'', Smart Materials and Structures Vol. 13, no.1, pp. 82--91, 2004.

[14] R. Kornbluh, R.Pelrine, J. Eckerle, and Joseph, "Electrostrictive polymer artificial muscles actuators", in IEEE International Conference on Robotics and Automation ,pp.2147-2154,1998.

[15] R. A. Schulte, ``The characteristics of the Pneumatic artificial muscle'', The Application of External Power in Prosthetics and Orthetics, Publ.874, Nas-RC, pp.94-115, 1962.

[16] Tondu, Bertrand, and Pierre Lopez. "Modeling and control of pneumatic artificial muscle robot actuators.", Control Systems, IEEE 20, no. 2, pp.15-38, 2000.

[17] H. K. Khalil, Nonlinear Systems, Maxwell Macmillan, 1992.